Spin density contribution to heavy ion potentials using different nucleonic densities

Manoj K. Sharma, Hemant Kumar, Rajeev K. Puri, and Raj K. Gupta
Centre of Advanced Study in Physics, Panjab University, Chandigarh 160014, India
(Received 10 March 1997)

Within the Skyrme energy density formalism, an analytical formula for the spin density part of the heavy ion interaction potential is obtained for $1s$-$0d$ shell nuclei by using the shell model density consistently. Comparisons are made with similar results for the parametrized Fermi density distribution which are useful for their later use in the calculations of fusion cross sections. [S0556-2813(97)04308-2]

PACS number(s): 24.10.−i, 21.60.Cs, 25.70.Jj, 27.20.+n

Recently, a lot of effort has been made to study the heavy ion potentials using the energy density formalism. In this renewed interest, the main stress is to understand the role of the spin density contribution to heavy ion potentials [1–7]. Two of us were the first to generalize the spin density part of the heavy ion interaction potential to unclosed shell nuclei [1]. The early derivations were made for closed j-shell nuclei only [8]. As a first application of this new formalism to unclosed shell nuclei [7], we had reported that the spin density part of the interaction potential can contribute towards the fusion barriers by as much as 1 MeV. This small effect can result in a decrease in the fusion cross section by $\sim$30 mb for Si+Si and $\sim$50 mb for Ni+Ni collisions [7]. In most of the calculations (including one in Ref. [7]), the shell-model (harmonic-oscillator) orbitals are used to define the spin density on the one hand and the parametrized Fermi density distributions are used for nucleon density on the other hand [1–7]. Thus all such calculations lack consistency. In our earlier work, the calculated spin density potentials for a couple of reactions like ^{12}C+^{12}C, ^{16}O+^{24}Mg, ^{24}Mg+^{36}Ar, and ^{40}Ca+^{90}Zr showed some differences for use of the full shell model and the Fermi densities [1]. Thus, in order to have a complete understanding of the roles of the shell density and Fermi density for evaluating the spin density potential, we need to study a large number of reactions and obtain a general behavior. A consistent study of the spin density part is very important. This study will pin down the importance of the spin density potential, if any. In other words, the aim of this paper is, at least, twofold: (i) to analyze a large number of collisions using the shell-model density consistently and to give a simple analytical formula for the spin density part of the interaction potential, and (ii) to compare the above said analytical results of shell density with the one which was obtained for the Fermi density. This study will reflect the differences between spin density potentials calculated by using two different nucleonic densities and hence the validity of the use of the Fermi density to evaluate the spin density contribution to heavy ion interaction potentials.

We present our results for some 50 collisions, involving ^{16}O to ^{40}Ca nuclei (i.e., $1s$-$0d$ shell; the contribution of the $1s$ shell towards the spin density is always zero). It may be relevant to point out here that the spin density part of the interaction potential is different for different (nl) shells [5] and hence an analytical formula for spin density part can be carried out for a given shell only. In the following, we first present our model briefly and then the results of our calculations. The details of the model can be found in Ref. [5].

In the Skyrme energy density formalism (SEDF), the interaction potential $V_N(R)$ is defined as the difference between the energy expectation value E of the colliding system at a finite separation distance R and at infinity,

$$V_N(R)=E(R)-E(\infty). \tag{1}$$

The two nuclei overlap at a distance R and are completely separated at infinity. The energy expectation value E for the energy density functional $H(\vec{r})$ of Vautherin and Brink [8] is given by

$$E=\int H(\vec{r})d\vec{r}, \tag{2}$$

where the Hamiltonian density $H(\vec{r})$ for an even-even spherical nucleus is given by

$$\begin{aligned}H(\rho,\tau,\vec{J})=&\frac{\hbar^2}{2m}\tau+\tfrac{1}{2}t_0[(1+\tfrac{1}{2}x_0)\rho^2-(x_0+\tfrac{1}{2})(\rho_n^2+\rho_p^2)]\\&+\tfrac{1}{4}(t_1+t_2)\rho\tau+\tfrac{1}{8}(t_2-t_1)(\rho_n\tau_n+\rho_p\tau_p)\\&+\tfrac{1}{16}(t_2-3t_1)\rho\nabla^2\rho+\tfrac{1}{32}(3t_1+t_2)\\&\times(\rho_n\nabla^2\rho_n+\rho_p\nabla^2\rho_p)+\tfrac{1}{4}t_3\rho_n\rho_p\rho\\&-\tfrac{1}{2}W_0(\rho\vec{\nabla}\cdot\vec{J}+\rho_n\vec{\nabla}\cdot\vec{J}_n+\rho_p\vec{\nabla}\cdot\vec{J}_p).\end{aligned} \tag{3}$$

Note that in Eq. (3) terms involving $\vec{J}^2$ have been neglected. Using Eqs. (1)–(3), the interaction potential is

$$V_N(R)=\int\{H(\rho,\tau,\vec{J})-H_1(\rho_1,\tau_1,\vec{J}_1)-H_2(\rho_2,\tau_2,\vec{J}_2)\}d\vec{r}. \tag{4}$$

Here ρ_i, τ_i, and $\vec{J}_i$ are the nucleon densities, kinetic energy densities, and the spin densities of individual nuclei, respectively, and using a sudden approximation, for a composite system $\rho=\rho_1+\rho_2$, $\tau=\tau_1+\tau_2$, and $\vec{J}=\vec{J}_1+\vec{J}_2$. For each nucleus $\rho_1=\rho_{n_1}+\rho_{p_1}$, $\rho_2=\rho_{n_2}+\rho_{p_2}$, $\tau_1=\tau_{n_1}+\tau_{p_1}$, $\tau_2=\tau_{n_2}+\tau_{p_2}$, $\vec{J}_1=\vec{J}_{n_1}+\vec{J}_{p_1}$, and $\vec{J}_2=\vec{J}_{n_2}+\vec{J}_{p_2}$ with subscripts n and p referring to neutrons and protons. The parameters x_0, t_0, t_1, t_2, t_3, and W_0, appearing in Eq. (3), have been fitted by several authors (see e.g., Ref. [5]) in a self-consistent manner to reproduce the correct single-particle properties of various nuclei. The different sets of parameters are labeled as S, SI, SII, SIII, etc., and in the present study we use the force SII, whose parameters are $x_0=0.34$, $t_0=(-)1169.90$ MeV fm^3, $t_1=585.60$ MeV fm^5, $t_2=-27.10$ MeV fm^5, $t_3=9331.10$ MeV fm^6, and $W_0=105.00$ MeV fm^5.

Each term in Hamiltonian (3) can be analyzed separately. For our discussion, we divide Eq. (4) into two parts, the spin-independent and spin-dependent parts, as

$$V_N(R)=V_P(R)+V_J(R), \tag{5}$$

with

$$V_P(R)=\int [H(\rho,\tau)-H_1(\rho_1,\tau_1)-H_2(\rho_2,\tau_2)]d\vec{r} \tag{6}$$

and

$$V_J(R)=\int [H(\rho,\vec{J})-H_1(\rho_1,\vec{J}_1)-H_2(\rho_2,\vec{J}_2)]d\vec{r}. \tag{7}$$

Note that $V_P(R)$ depends on the nucleon and kinetic energy densities, whereas $V_J(R)$ depends on the nucleon and spin densities. In the following, we focus only on $V_J(R)$ and use both the shell-model and Fermi-type densities for ρ_i in Eq. (7).

From Eqs. (3)–(7), the spin density potential reads as

$$V_J(R)=-\frac{3}{4}W_0\int [\rho_1(\vec{\nabla}\cdot\vec{J}_2)+\rho_2(\vec{\nabla}\cdot\vec{J}_1)]d\vec{r}. \tag{8}$$

In terms of single-particle orbitals that define a Slater determinant ϕ_i, the spin density for $q=n$ or p is given as

$$\vec{J}_q(\vec{r})=(-i)\sum_{i,s,s'}\phi_i^*(\vec{r},s,q)[\nabla\phi_i(\vec{r},s',q)\times\langle s|\vec{\sigma}|s'\rangle]. \tag{9}$$

Here the summation i runs over all the occupied single-particle orbitals and s and q are, respectively, the spin and isospin indices. Since any self-consistent calculation is very time consuming, Eq. (9) is solved by using the ansatz [8]

$$\phi_i(\vec{r},s,q)=[R_\alpha(r)/r]y_{ljm}(\hat{r},s)\chi_q(t), \tag{10}$$

where

$$y_{ljm}(\hat{r},s)=\sum_{m_l m_s}\langle l\tfrac{1}{2}m_l m_s|jm\rangle Y_l^{m_l}(\hat{r})\chi_{m_s}(s) \tag{11}$$

and $\chi_q(t)$ is the isospin part of the wave function. The index α $(=q,n,l)$ specifies the radial part of the wave function, $R_\alpha(r)$. For a completely filled j shell for n or p, Eq. (9) reduces to

$$\vec{J}_q^c(\vec{r})=\frac{\vec{r}}{4\pi r^4}\sum_\alpha (2j_\alpha+1) \times[j_\alpha(j_\alpha+1)-l_\alpha(l_\alpha+1)-\tfrac{3}{4}]R_\alpha^2(\vec{r}). \tag{12}$$

Note that $\vec{J}_q^c=0$ for a completely filled pairs of orbitals with $j=l+\frac{1}{2}$ and $j=l-\frac{1}{2}$.

For an even-even nucleus with valence particles (or holes) outside (inside) the closed j shell, we divide the contribution to $\vec{J}_q(\vec{r})$ in two parts [5]: one due to the core consisting of closed shells and another due to the valence n_v particles (or holes),

$$\vec{J}_q(\vec{r})=\vec{J}_q^c(\vec{r})\pm\vec{J}_q^{n_v}(\vec{r}). \tag{13}$$

The (+) sign is for particles and (−) sign is for holes. The first term is the same as Eq. (12) and the second term reads as [1]

$$\vec{J}_q^{n_v}=\frac{n_v\vec{r}}{4\pi r^4}\left[j(j+1)-l(l+1)-\frac{3}{4}\right]R_l^2(r). \tag{14}$$

The normalized radial wave function $R_{nl}(r)$ in Eqs. (10), (12), and (14) is taken from the shell model [9], which is based on harmonic oscillator calculations:

$$R_{nl}(r)=\left[\frac{2^{l-n+2}(2\nu)^{l+3/2}(2l+2n+1)!!}{\sqrt{\pi}[(2l+1)!!]^2 n!}\right]^{1/2} \times r^{l+1}e^{-\nu r^2}v_{nl}(2\nu r^2), \tag{15}$$

where

$$v_{nl}(x)=\sum_{k=0}^{n}(-1)^k 2^k\begin{bmatrix} n\\ k\end{bmatrix}\frac{(2l+1)!!}{(2l+2k+1)!!}x^k \tag{16}$$

and the scale factor ν, related to oscillator parameter b, is

$$\nu=\frac{1}{2b^2}=\frac{m\omega}{2\hbar}\ \ (\text{in fm}^{-2}), \tag{17}$$

with

$$\hbar\omega=41A^{-1/3}.$$

For more details, we refer the reader to Refs. [1,5]. For nucleonic density, appearing in Eq. (8), we use two different forms.

(i) *Shell density.* For a consistent evaluation of the spin density part of the interaction potential, we construct the nucleon-density using shell model wave functions as

$$\rho_i^{\mathrm{SD}}(\vec{r})=\sum_{i,s}|\phi_i(\vec{r},s,q)|^2, \tag{18}$$

where the sum i runs over all occupied levels. In other words, Eq. (18) represents the density for a completely closed shell with both $j=l\pm\frac{1}{2}$ filled. For nuclei with even n_ν valence particles (or holes), Eq. (18) is generalized to [1]

$$\rho^{\mathrm{SD}}(\vec{r})=\begin{cases}\rho_{cc}(\vec{r})+\dfrac{(2j+1)}{2(2l+1)}|\phi_{nlj}(\vec{r},s,q)|^2 & (\text{for closed } j \text{ shell}),\\[2ex] \rho_c(\vec{r})\pm\dfrac{n_v}{2(2l+1)}|\phi_{nlj}(\vec{r},s,q)|^2 & (\text{for } n_v \text{ valence particles}).\end{cases} \tag{19}$$

Here $\rho_{cc}(\vec{r})$ is the nucleon density distribution due to the closed major shell as core [Eq. (18)] and $\rho_c(\vec{r})$ is the nucleon

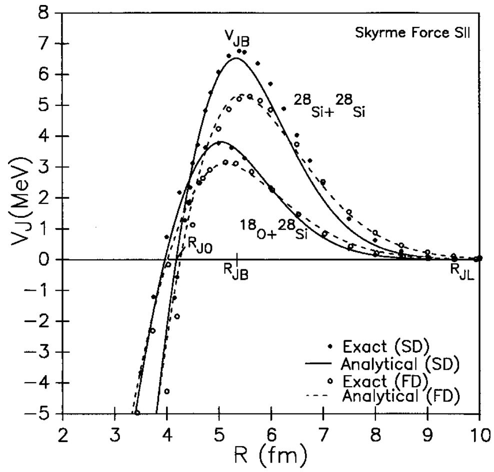

FIG. 1. Spin density part of the heavy ion interaction potential V_J using Skyrme force SII, as a function of separation distance R for $^{28}Si+^{28}Si$ and $^{18}O+^{28}Si$ reactions. The solid and open circles are the exact calculations whereas the solid and dashed lines are the analytical calculations using Eq. (27), respectively, with Eqs. (22)–(25) and (28)–(31) for the shell-model and Fermi density. The height V_{JB}, position R_{JB}, and other coordinates R_{J0} and R_{JL} of the spin density potential are also indicated for one case.

density due to closed major shell or closed j shell, depending on whether the valence nucleons are outside the major-shell core or closed j shell.

(ii) *Fermi density.* The Fermi density distribution is given by

$$\rho^{\mathrm{FD}}(r_i)=\rho_{0i}\{1+\exp[(r_i-R_{0i})/a_i]\}^{-1}, \quad i=1,2, \tag{20}$$

with

$$r_2=[r_1^2+R^2-2r_1R\cos\theta]^{1/2} \quad \text{for } 0\leqslant r\leqslant\infty. \tag{21}$$

Here R_{0i} and a_i are the half density radii and surface thickness parameters, respectively, taken from Ref. [1] and R is the separation distance of two nuclei from their centers.

The two different forms of nucleon density distributions will give us a unique possibility of analyzing the role of different densities, the shell-model density being a more consistent choice in the present study. In other words, the validity of the Fermi density distribution to heavy ion interaction potentials, including the spin density part, will be tested.

Figure 1 shows the spin density potentials $V_J(R)$ for collisions of $^{28}Si+^{28}Si$ and $^{18}O+^{28}Si$ using shell density (SD) and Fermi density (FD) distributions (the solid and open circles, marked exact). We find that though both SD and FD densities show quite a similar behavior of being repulsive at larger distances and attractive at smaller distances: there are important differences in the interaction potentials. For the study of heavy ion collisions, the relevant part of the potential is one beyond the repulsive maximum. The repulsive maximum is much larger for the shell density than for the Fermi density. Also, in the surface region, the shell density potential is weaker than the Fermi density potential.

The reactions presented here are just a couple of examples. To have a general comparison between the spin density potential obtained using the shell density and Fermi density, we need to obtain a parametrized form of the spin density part of the heavy ion potential using the shell density.

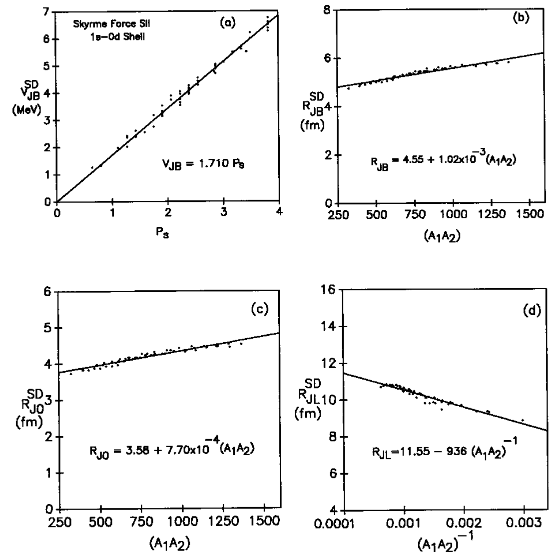

FIG. 2. Plots of V_{JB} vs P_s, R_{JB}, and R_{J0} vs $A_1\cdot A_2$ and R_{JL} vs $(A_1\cdot A_2)^{-1}$ for $1s$-$0d$ shell nuclei using Skyrme force SII with the shell density. The exact calculations are shown by solid circles whereas solid lines give analytical fits to their average behaviors.

Following [5], we parametrize the spin density part of the heavy ion interaction potential based on shell density, in terms of four points, namely, (i) the height of the repulsive maximum V_{JB}, (ii) the position R_{JB} of V_{JB}, (iii) the position R_{J0} where the spin density potential changes its nature from repulsive to attractive and hence V_J becomes zero at R_{J0} for a moment, and (iv) the limiting distance R_{JL} where $V_J(R)$ goes to zero. For practical purposes, we fix R_{JL} as the distance where $V_{JL}=0.003$ MeV, instead of zero. By analyzing more than 50 reactions from $1s$-$0d$ shell, as depicted in Fig. 2, one can obtain the general equation for V_{JB}, R_{JB}, R_{J0}, and R_{JL} as

$$V_{JB}^{\mathrm{SD}}=1.710P_s, \tag{22}$$

$$R_{JB}^{\mathrm{SD}}=4.55+(1.02\times10^{-3})A_1\cdot A_2, \tag{23}$$

$$R_{J0}^{\mathrm{SD}}=3.58+(7.70\times10^{-4})A_1\cdot A_2, \tag{24}$$

$$R_{JL}^{\mathrm{SD}}=11.55-936(A_1-A_2)^{-1}, \tag{25}$$

where the particle strength

$$P_s=\sum_\alpha \frac{(2j_\alpha+1)}{4\pi}\left[j_\alpha(j_\alpha+1)-l_\alpha(l_\alpha+1)-\frac{3}{4}\right] \pm\frac{n_v}{4\pi}\left[j(j+1)-l(l+1)-\frac{3}{4}\right]. \tag{26}$$

Using these four equations for V_{JB}, R_{JB}, R_{J0}, and R_{JL}, one can generate the spin density part of heavy ion interaction potential by

$$V_J(R)=\begin{cases} V_{JB}\exp\left[\ln\left[\frac{V_{JL}}{V_{JB}}\right]\left(\frac{R-R_{JB}}{R_{JL}-R_{JB}}\right)^{5/3}\right] & \text{for } R\geqslant R_{JB}, \\ V_{JB}-V_{JB}\left(\frac{R-R_{JB}}{R_{J0}-R_{JB}}\right)^2 & \text{for } R\leqslant R_{JB}. \end{cases} \tag{27}$$

A similar fit was obtained for Fermi density for the $1s$-$0d$ shell nuclei [5], with

$$V_{JB}^{\rm FD}=1.4006P_s, \qquad (28)$$

$$R_{JB}^{\rm FD}=4.58+(1.11\times 10^{-3})A_1\cdot A_2, \qquad (29)$$

$$R_{J0}^{\rm FD}=3.58+(8.70\times 10^{-4})A_1\cdot A_2, \qquad (30)$$

$$R_{JL}^{\rm FD}=12.77-1129(A_1\cdot A_2)^{-1}. \qquad (31)$$

A comparison between the exact calculations of spin density potential and the analytical fit [Eq. (27) with Eqs. (22)–(25) for SD and Eqs. (28)–(31) for FD] is also shown in Fig. 1. We notice that the spin density part of heavy ion potential is parametrized as nicely for the shell-model density as for the Fermi density.

Finally, to figure out the difference between the spin density potentials using shell density and Fermi density, we calculate the percentage deviation

$$\Delta^i(\%)=\left|\frac{i^{\rm FD}-i^{\rm SD}}{i^{\rm FD}}\right|\times 100, \qquad (32)$$

where i stands for V_{JB}, R_{JB}, R_{J0}, and R_{JL}. This quantity gives the difference of results between the shell density and Fermi density. Figure 3 shows the variation of Δ for V_{JB} and R_{JB}, R_{J0}, and R_{JL}, respectively, as a function of P_s and $(A_1\cdot A_2)$. The following interesting results are evident.

(i) The value of repulsive maximum recorded for the shell-model density is $\sim$22% more than for the Fermi density. Thus, using the shell-model density, the spin density part of the heavy ion potential is $\sim\frac{1}{5}$th more repulsive than using the Fermi density.

(ii) The variations of Δ for R_{JB}, R_{J0}, and R_{JL} with $(A_1\cdot A_2)$ also present an interesting result. The shell density has negligible effect on R_{JB} and R_{J0}, whereas it results in about 8% effect for R_{JL}. It is relevant to mention here that the errors in fixing R_{JL} are quite large (see, e.g., Fig. 13 of Ref. [5]). Therefore, one should not take the variation of R_{JL} for the shell density so seriously.

From our analysis (of involving about 50 reactions belonging to the $1s$-$0d$ shell), it is clear that the use of the shell density (compared to the Fermi density) for calculating the spin density part of the heavy ion interaction potential results in a $\sim$22% enhancement in the repulsive maximum, the barrier height V_{JB}. The interesting aspect of this result is that it is independent of the size of colliding nuclei, within this shell. Furthermore, since the position coordinates R_{JB}, R_{J0}, and R_{JL} are nearly independent of the nature of nucleon density used, the barrier position and range of the spin density part of the heavy ion potential are independent of the nature of the nucleon density.

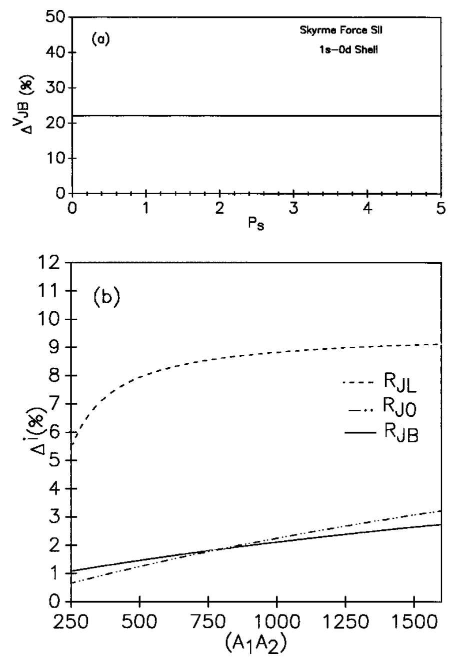

FIG. 3. Percentage difference $\Delta^i(\%)=|(i^{\rm FD}-i^{\rm SD})/i^{\rm FD}|\times 100\%$, with $i=V_{JB}$ and R_{JB}, R_{J0}, and R_{JL}, respectively, as a function of P_s and $(A_1\cdot A_2)$.

In summary, we have studied the role of different nucleon densities on the spin density part of the interaction potential, employing the shell model density and the two-parameter Fermi density. A simple analytical formula of the spin density part of the interaction potential, using the shell density, is obtained and the same is compared with that for the Fermi density. We find that the shell density yields a $\sim$22% more repulsive spin density barrier as compared to the one given by the Fermi density. In the surface region, however, the spin density potential for the shell density is lower than that for the Fermi density. In other words, the magnitude of the spin density part of the heavy ion potential is strongly influenced by the nature of the nucleon density used, whereas the maxima position and range are independent of the nature of the density used.

This work is supported in part by the Department of Science and Technology, Government of India.

[1] R. K. Puri, P. Chattopadhyay, and R. K. Gupta, Phys. Rev. C **43**, 315 (1991).
[2] K. C. Panda, J. Phys. G **11**, 1323 (1985); K. C. Panda and T. Patra, *ibid.* **14**, 1489 (1988).
[3] S. Kaur and P. Chattopadhyay, Phys. Rev. C **36**, 1016 (1987).
[4] Li Guo-Qiang and Xu Gong-Ou, Nucl. Phys. **A492**, 340 (1989).
[5] R. K. Puri and R. K. Gupta, Int. J. Mod. Phys. E **1**, 269 (1992).
[6] R.K. Puri and R. K. Gupta, Phys. Rev. C **51**, 1568 (1995).
[7] R. K. Puri and R. K. Gupta, Phys. Rev. C **45**, 1837 (1992).
[8] D. Vautherin and D. M. Brink, Phys. Rev. C **5**, 626 (1972).
[9] A. de Shalit and I. Talmi, *Nuclear Shell Theory* (Academic, New York, 1963).